

# First lidar observations of mesospheric hydroxyl

E.J. Brinksma<sup>1</sup>, Y.J. Meijer<sup>1</sup>, I.S. McDermid<sup>2</sup>, R.P. Cageo<sup>2</sup>, J.B. Bergwerff<sup>3</sup>, D.P.J. Swart<sup>3</sup>, W. Ubachs<sup>1</sup>, W.A. Matthews<sup>4</sup>, W. Hogervorst<sup>1</sup>, J.W. Hovenier<sup>1</sup>

**Abstract.** Ground-based lidars have been used to detect and identify ground-state ( $v''=0$ ) hydroxyl radicals (OH) in the mesosphere between about 75 and 85 km altitude. These lidars operate near 308 nm and OH is observed through laser-induced-fluorescence on the  $A^2\Sigma^+ - X^2\Pi(0,0)$  band. The results expose a valuable global set of nighttime OH observations, since existing long-term lidar data at several NDSC sites contain the (serendipitous) OH information. Results of lidar observations are presented from two mid-latitude sites, one in each hemisphere: Table Mountain (34°N), California, and Lauder (45°S), New Zealand. They show observations of a geometrically thin ( $\sim 3$  km) nocturnal layer of OH near 80 km. For the Table Mountain observations, the derived values for the OH density at 80 km typically are  $2 - 4 \times 10^5 \text{ cm}^{-3}$  which is in accordance with model predictions [Dodd *et al.*, 1994]. The temporal behavior of the mesospheric OH signal, following sunset, that was found, supports previous model predictions [Allen *et al.*, 1984] in a qualitative fashion.

## Introduction

Despite the pivotal role that hydroxyl radicals play in atmospheric chemistry, measurements of OH are difficult and sparse. Lidar measurements of OH in the mesosphere would be valuable, for example, to confirm model predictions and to track an important part of the mesospheric ozone and water budget (for a recent discussion see Summers *et al.* [1997]).

Nighttime lidar measurements could complement the few rocket-based or space borne measurements of ground-state OH in the high mesosphere which have been performed during daytime [Anderson, 1971a; 1971b; ; Morgan *et al.*, 1993; Conway *et al.*, 1996], as well as the observations of OH night-glow caused by transitions between high vibrational states (observed in the Meinel bands).

## Observations

Several groups operating XeCl excimer laser based DIAL systems within the Network for the Detection of Strato-

<sup>1</sup>Faculty of Physics and Astronomy, Vrije Universiteit, Amsterdam, The Netherlands.

<sup>2</sup>Jet Propulsion Laboratory, California Institute of Technology, Table Mountain Facility, Wrightwood.

<sup>3</sup>National Institute of Public Health and the Environment (RIVM), Air Research Laboratory, Bilthoven, The Netherlands.

<sup>4</sup>National Institute of Water and Atmospheric Research Ltd. (NIWA), Lauder, New Zealand

Copyright 1998 by the American Geophysical Union.

Paper number 97GL53561  
0094-8534/97/97GL-53561\$05.00

spheric Change (NDSC), have observed peaks near 80 km in the 308 nm lidar return signals. These signals have been measured and archived routinely, for many years, for the purpose of ozone profiling, but until now the source or cause of these peaks had not been determined. These peaks were first observed at Table Mountain in 1989. Here, we present substantial evidence that these peaks are caused by laser-induced-fluorescence (LIF) by mesospheric OH.

An observation by the RIVM lidar (for a system description see Swart *et al.* [1994]), located in Lauder, New Zealand, 45°S, 170°E, in which the peak stands out clearly, is shown in Figure 1. The RIVM XeCl laser operates in a 'free running' mode, i.e., the laser light is emitted in a relatively broad spectrum centered at 308 nm (emission bandwidth typically 0.5 nm), which overlaps several OH absorption transitions within the  $A^2\Sigma^+ - X^2\Pi(0,0)$  band. Absorption in these lines gives rise to fluorescence in the (0,0) band resulting in enhanced return signals in the 308 nm spectral region. The observation that peaks only appear in the 308 nm channel, and not in the 353 nm channel (Figure 1) rules out scattering (by, e.g., mesospheric clouds) as the underlying process. The excited  $A^2\Sigma^+, v=0$  state lifetime is 0.7  $\mu\text{s}$ . Compared to the lidar resolution of 2  $\mu\text{s}$  (equivalent to 300 m) the fluorescence lifetime causes only little smearing of the altitude determination of the observed peaks.

For the Lauder site, the observed OH layer is situated at 80 to 85 km altitude, and is geometrically thin (FWHM

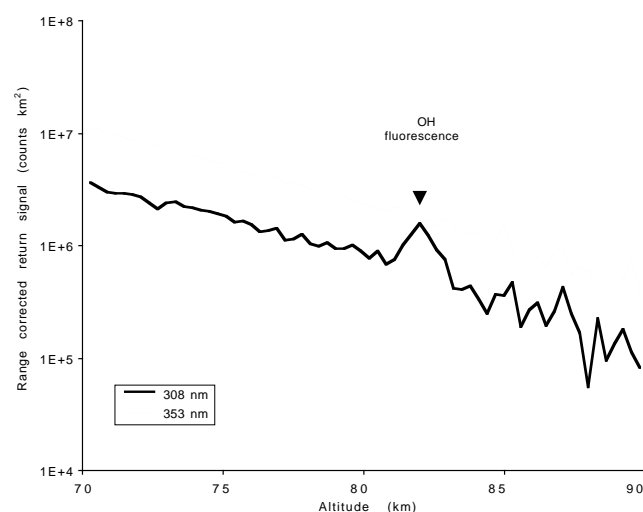


**Figure 1.** Range corrected lidar return signals near 308 and 353 nm, as measured by the RIVM stratospheric lidar, Lauder, New Zealand, on March 10, 1997, at 9.30 PM local time. Note that near an altitude of 82 km a signal peak is present in the 308 nm channel, but absent in the simultaneously measured 353 nm channel.

of about 3 km). Both the shape and the altitude of the observed feature differ from night to night, and frequently the feature is not observed. The results are in accordance with model calculations [Allen *et al.*, 1984], which predicted that the nighttime OH number density profile should peak sharply at about 80 km, at mid-latitudes, due to nighttime recombination at lower altitudes.

Other ozone lidar groups within the NDSC, operating similar lidar systems, were surveyed to determine the extent of observations. Those confirming observation of the OH feature include the JPL lidars at Mauna Loa, HI and Table Mountain, CA; the GSFC mobile system, STROZ-LITE (T. McGee, personal communication, 1996); the CRESTech lidars in Toronto and Eureka, Canada (W. Steinbrecht and D. Donovan, personal communication, 1996); the DWD lidar at Hohenpeissenberg, Germany (W. Steinbrecht, personal communication, 1996); the NILU lidar at ALOMAR, Andoya, Norway (D. Rees and G. Hansen, personal communication, 1997), and the NIES lidar in Tsukuba, Japan (H. Nakane, personal communication, 1997).

## Experimental Verification

Experiments proving that the lidar systems are indeed observing OH were performed using the JPL-TMF lidar at Table Mountain, California (for a system description see [McDermid *et al.*, 1990]) but hold implications for all stratospheric ozone lidars. The JPL-TMF lidar usually operates in 'line-narrowed mode', where a tunable injection laser is used to seed and lock the wavelength of the amplifying laser. The resulting XeCl laser output is tunable in the range from 307.8 to 308.3 nm, although not continuously, and typically has a bandwidth of about 0.008 nm.

The laser light was first directed through a propane flame, which is a source of OH, and the fluorescence intensity in a direction perpendicular to the laser beam was registered as a function of laser wavelength. This spectrum provided a precise calibration of the laser wavelength and bandwidth. The (merged)  $P_1(1)/Q_{21}(3)$  doublet at 308.16 nm was partially resolved from the  $Q_1(3)$  line at 308.15 nm confirming the bandwidth estimate of 0.008 nm. The laser was then directed into the atmosphere, and alternately tuned on and off the peak absorption using the laboratory experiment wavelength calibration. The results are presented in Figure 2. Clearly, when the laser was tuned to the wavelength of an OH transition a peak was present in the lidar return and when it was tuned off it was not. This strongly indicates that the observed peaks are caused by laser-induced fluorescence from OH.

## OH Number Density Derivation From the Table Mountain Observations

The OH concentrations will be derived directly from the LIF signals, which has been considered previously for tropospheric and stratospheric measurements [McDermid *et al.*, 1983a; 1983b, ]. Here, the observed OH LIF signal from the JPL-TMF lidar will be compared to the Rayleigh background retrieved at the same wavelength. Two major assumptions are made. Firstly, collisional quenching of the excited state population is neglected, which in view of the typical pressure at 80 km altitude ( $\sim 5 \times 10^{-3}$  hPa) and the fluorescent rate of  $1.4 \times 10^6 \text{ s}^{-1}$  is justified. Secondly, local thermodynamic equilibrium (LTE) is assumed, at prevailing

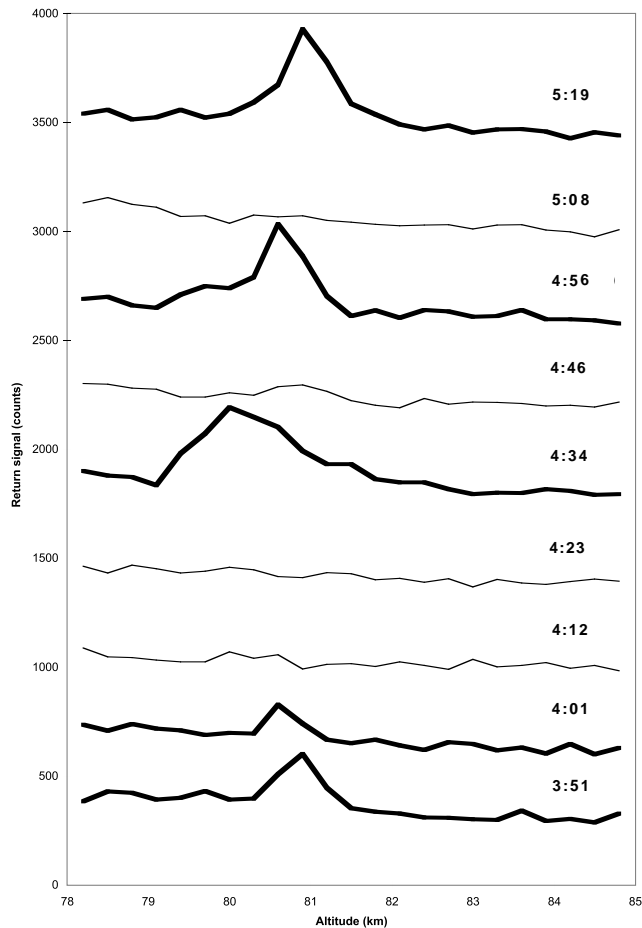


**Figure 2.** Lidar return signals observed by the JPL-TMF lidar system, on August 9, 1996, showing that the OH feature is present in the 'ON' wavelength (bold lines, 308.1 nm) but absent in the 'OFF' wavelength (thin lines, 307.9 nm). All measurements are integrated over 10 minutes, and are labeled with the time of observation (UT). Astronomical sunset was at 2:53 UT. For clarity, the signal-counts for the consecutive measurements have been successively offset by 400 counts.

temperatures of 180 to 210 K. Furthermore, the following approximations are made: Firstly, absorption in the  $Q_{21}(3)$  satellite line is negligible compared to the stronger  $P_1(1)$  line, which induces fluorescence in the  $P_1(1)$ ,  $P_{12}(1)$  and  $O_{12}(1)$  lines. These are detected with the same efficiency. Secondly, in view of the Franck-Condon factors of the A-X system, only fluorescence in the resonant (0,0) band is considered. And thirdly, an expression for the angular distribution of the fluorescence is assumed. Usually, this is taken to be isotropic. However, OH molecules are excited in a rotationless state ( $N=0$ ) with the transition dipole moments in the plane of the polarization. 60 % of this state decays via a single  $P_1(1)$  line (according to the Einstein A coefficients from Cageao *et al.* [1997]), yielding enhanced forward-backward anisotropy. We assume the same enhancement as for Rayleigh scattering, although the effect is counteracted by the contribution of the spin-flipping transitions  $P_{12}(1)$  and  $O_{12}(1)$ . This assumption may lead to an underestimation of the OH density by up to 50 %. With the above

assumptions and approximations, the lidar equations for the OH and Rayleigh signals are:

$$r^2 I_{OH} = C P_{N=1} N_{OH} \int \frac{3\sigma_{P(1)}(\nu)}{8\pi} g^{OH}(\nu) \eta(\nu) d\nu \quad (1)$$

$$r^2 I_{Ray} = C N_{air} \int \frac{3\sigma_{Ray}(\nu)}{8\pi} g^L(\nu) \eta(\nu) d\nu \quad (2)$$

$r$	altitude,
$I_{OH}$	observed LIF signal intensity,
$C$	a constant comprising lidar system parameters,
$P_{N=1}$	fractional population of OH molecules in the ${}^2\Pi_{3/2}$ N=1 level,
$N_{OH}$	OH number density,
$\sigma_{P(1)}$	absorption cross section,
$\nu$	frequency,
$g^{OH}$	convolution of the $P_1(1)$ lineshape with the laser profile,
$\eta$	detector spectral transmission,
$I_{Ray}$	observed Rayleigh signal intensity,
$N_{air}$	air number density ,
$\sigma_{Ray}$	cross section for Rayleigh extinction,
$g^L(\nu)$	convolution of the Rayleigh spectral extinction with the laser profile.

The integrated absorption cross section is calculated by multiplying the integral of the effective fluorescence cross section,  $\sigma_f$ , by the Hönl-London factor for the  $P_1(1)$  line which amounts to 0.294.  $\sigma_f$  is calculated using equation 3[Svelto, 1989].

$$\sigma_f(\nu) = \frac{\lambda_0^2}{8\pi} A g^{OH}(\nu) \quad (3)$$

The rate A is the inverse of the excited state lifetime of the  $v=0$  level ( $690 \pm 70$  ns, [German, 1975]). At T=200 K, the line profile  $g^{OH}(\nu)$  has a Doppler width of  $\Delta\nu_D = 7.6 \times 10^{-4}$  nm. This yields an integrated absorption cross section of  $6.3 \times 10^{-15}$  cm<sup>2</sup>.

In LTE and at typical temperatures of 180 to 210 K, the fractional population of the probed  ${}^2\Pi_{3/2}$  N=1 level is 15%. An expression for the OH number density (summed over all vibrational and rotational levels) is found by dividing eq. 1 by eq. 2 and by evaluating the frequency profiles. Also using  $\sigma_{Ray} = 5 \times 10^{-26}$  cm<sup>2</sup> we find:

$$N_{OH} = 5.3 \times 10^{-11} N_{air} \frac{I_{OH} \Delta\nu_L}{I_{Ray} \Delta\nu_D} \quad (4)$$

Typically,  $N_{air} = 4 \times 10^{14}$  cm<sup>-3</sup>,  $\Delta\nu_L = 8 \times 10^{-3}$  nm and  $\Delta\nu_D = 7.6 \times 10^{-4}$  nm. From the lidar signal, the ratio of the LIF signal over the Rayleigh-scattered signal is determined. This ratio is typically between one and two, with strong variability from night-to-night as discussed previously, implying an OH number density of  $2 - 4 \times 10^5$  cm<sup>-3</sup>.

A kinetic model for state-to-state dynamics of OH (v,J) [Dodd et al., 1994] predicts that the nighttime OH number density is in the range of  $1 - 2 \times 10^5$  cm<sup>-3</sup> at altitudes near 85 km, where a maximum is obtained. This model is based on an analysis of infrared airglow data, retrieved by the Space Shuttleborne CIRRS 1A instrument, and yields significant deviations from LTE for high vibrational and rotational states. However, the OH at altitudes near 85 km

exists mainly in the  ${}^2\Pi, v=0, N=1-7$  states, and non-LTE effects contribute less than 20 % to the OH density in this model. The OH density presented by Dodd et al. agrees to our findings of  $2 - 4 \times 10^5$  cm<sup>-3</sup> within a factor of two. In the light of the assumptions used, the estimated uncertainty in the lidar-derived OH number density is about a factor of two or three, which makes the agreement satisfactory. Dodd et al. find an altitude of 85 km for the OH peak density, somewhat higher than our findings, which are that the peaks occur between 75 and 85 km, varying from night-to-night.

Most NDSC stratospheric lidar systems, including the RIVM lidar, employ lasers operating in free-running mode, as opposed to the line-narrowed mode that was used for the measurements interpreted above. For those systems, multiple absorption bands give rise to laser-induced-fluorescence, and derivation of an OH number density is difficult. There are, e.g., uncertainties in the convolution of the broad laser spectral transmission with the OH absorption spectrum, as well as uncertainties in the lidar detector spectral transmission. The magnitude of the observed signals is, however, directly proportional to the OH density, and therefore these data potentially provide useful information about mesospheric OH.

## Example

Figure 3 shows a series of consecutive measurements of the OH feature, taken shortly after sunset, by the JPL-TMF lidar. The temporal behavior of the OH concentration in the first two hours after sunset is shown. The initial rise, the following decline, as well as the altitude shift of the OH peak concentration during the night all are in accord with model predictions [Allen et al., 1984]. After the first  $\sim 2$  hours after sunset, the OH peak reaches an essentially constant level, which is approximately 10% of the maximum level observed earlier, and it remains at the same altitude

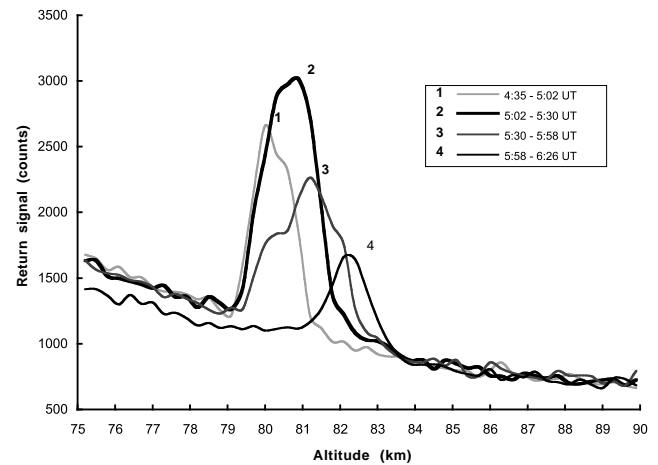


**Figure 3.** Consecutive (background-corrected) observations of the OH peaks, expressed in terms of the ratio of the OH signal and the fitted Rayleigh background (left axis). The right axis represents the order-of-magnitude estimate of the corresponding OH number densities. These observations were performed on July 17, 1996, using the JPL-TMF lidar system. The observations were performed shortly after sunset, with an integration time of 28 minutes each.

throughout the night. We have not observed any changes in the OH concentration or altitude distribution in the period immediately before sunrise.

Similar temporal behavior has been observed at the TMF site during other nights in July and August of 1996, as well as over Lauder, New Zealand on several occasions, although the initial rise in concentrations is not always present.

## Conclusions

A new method to retrieve information about mesospheric OH from existing lidar signals has been presented. The first results show that a nocturnal layer of ground-state OH is frequently observable in the high mesosphere at many sites around the world. Approximate OH number densities derived from the observations performed at Table Mountain are in accord with model calculations [Dodd *et al.*, 1994]. A series of consecutive lidar measurements, following sunset and throughout the night, shows the temporal behavior of this layer which conforms with model predictions [Allen *et al.*, 1984]. Most of the stratospheric lidar systems within the NDSC employ lasers that are limited to operating in 'broad band' mode, which makes the derivation of absolute OH number densities difficult. However, their observations are capable of showing qualitatively the nighttime behavior of OH ( $v''=0$ ) which has not been observed by other instruments.

**Acknowledgments.** We are indebted to Dr. J.F. de Haan, Dr. S. Madronich and colleagues at NIWA Lauder, New Zealand for useful discussions. M. Schmoë, Dr. T. Leblanc and K.F. Boersma are thanked for performing some of the measurements described. An anonymous referee's contribution to the quantification of the measurements is acknowledged. This work was carried out, in part, at the Jet Propulsion Laboratory, California Institute of Technology, under an agreement with the National Aeronautics and Space Administration.

## References

- Allen, M., J.I. Lunine, and Y.L. Yung, The Vertical Distribution of Ozone in the Mesosphere and Lower Thermosphere, *J. Geophys. Res.*, 89, D3, 4841-4872, 1984.
- Anderson, J.G., Rocket-borne ultraviolet spectrometer measurement of OH resonance fluorescence with a diffusive transport model for mesospheric photochemistry, *J. Geophys. Res.*, 76, 4634-4652, 1971.
- Anderson, J.G., Rocket measurements of OH in the mesosphere, *J. Geophys. Res.*, 76, 7820-7824, 1971.
- Cageao, R.P., Y.L. Ha, Y. Jiang, M.F. Morgan, Y.L. Yung, and S.P. Sander, Calculated hydroxyl  $A^2\Sigma - X^2\Pi(0,0)$  band emission rate factors applicable to atmospheric spectroscopy, *J. Quant. Spectrosc. Radiat. Transfer*, 57 no. 5, 703-717, 1997.
- Conway, R.R., M.H. Stevens, J.G. Cardon, S.E. Zasadil, C.M. Brown, J.S. Morrill, and G.H. Mount, Satellite measurements of hydroxyl in the mesosphere, *Geophys. Res. Lett.*, 23, 16, 2093-2096, 1996.
- Demtröder, W.: *Laser Spectroscopy*, Springer-Verlag Heidelberg New York, 1982.
- Dodd, J.A., S.J. Lipson, J.R. Lowell, P.S. Armstrong, W.A.M. Blumberg, R.M. Nadile, S.M. Adler-Golden, W.J. Marinelli, K.W. Holtzclaw, and D.B. Green, Analysis of hydroxyl earth-limb emission: Kinetic model for state-to-state dynamics of OH, *J. Geophys. Res.*, 99, 3559-3585, 1994.
- German, K.R., Radiative and Predissociative lifetimes of the  $v''=0, 1$  and 2 levels of the  $A^2\Sigma^+$  state of OH and OD, *J. Chem. Phys.*, 63, 5252-5255, 1975.
- McDermid, I.S., J.B. Laudenslager, and T.J. Pacala, The Hydroxyl Radical: Verification of LIDAR Experiment, *JPL Document D-493*, 1983.
- McDermid, I.S., J.B. Laudenslager, and T.J. Pacala, New Technological developments for the remote detection of atmospheric hydroxyl radicals, *Appl. Opt.*, 22, 2586-2591, 1983.
- McDermid, I.S., S.M. Godin, and L.O. Lindquist, Ground-based laser DIAL system for long-term measurements of stratospheric ozone, *Appl. Opt.*, 29, 3603, 1990.
- Morgan, M.F., D.G. Torr, M.R. Torr, Preliminary measurements of mesospheric OH  $X^2\Pi$  by ISO on Atlas 1, *Geophys. Res. Lett.*, 20, 6, 511-514, 1993.
- Summers, M.E., R.R. Conway, D.E. Siskind, M.H. Stevens, D. Offermann, M. Riese, P. Preusse, D.F. Strobel, J.M. Russel III, Implications of Satellite OH Observations for Middle Atmospheric  $H_2O$  and Ozone, *Science*, 277, 1967-1970, 1997.
- Svelto, O.: *Principles of Lasers*, 3rd edition, Plenum Press, New York, 1989.
- Swart, Daan P.J., Jan Spakman, and Hans B. Bergwerff: RIVM's Stratospheric Ozone Lidar for NDSC Station Lauder: System Description and First Results. Abstracts of Papers of the 17th International Laser Radar Conference, Sendai, Japan, 405-408, 1994.

---

E.J. Brinksma (email: ellen@nat.vu.nl), W. Hogervorst, J.W. Hovenier, Y.J. Meijer, W. Ubachs, Vrije Universiteit, Faculty of Physics & Astronomy, De Boelelaan 1081, 1081 HV Amsterdam, The Netherlands.

R.P. Cageao, I.S. McDermid, Jet Propulsion Laboratory (JPL), California Institute of Technology, Table Mountain Facility, Wrightwood, CA 92397

J.B. Bergwerff, D.P.J. Swart, National Institute of Public Health and the Environment (RIVM), Air Research Laboratory, P.O. Box 1, 3720 BA Bilthoven, The Netherlands.

W.A. Matthews, National Institute of Water and Atmospheric Research Ltd. (NIWA), Private Bag 50061, Omakau, Central Otago, New Zealand

(Received June 24, 1997; revised November 19, 1997; accepted November 24, 1997.)